2021

Environmental Modifications of Atomic Properties: The Ground and 1s2p Excited States of Compressed Helium

N. C. Pyper

T. C. Naginey

Colm T. Whelan
Old Dominion University, cwhelan@odu.edu

Original Publication Citation

Pyper, N. C., Naginey, T. C., & Whelan, C. T. (2021). Environmental modifications of atomic properties: The ground and 1s2p excited states of compressed helium. *The Journal of Chemical Physics, 155*(21), 1-14, Article 214301. https://doi.org/10.1063/5.0066626

The Journal of Chemical Physics ARTICLE scitation.org/journal/jcp

Environmental modifications of atomic properties: The ground and 1*s*2*p* excited states of compressed helium

Cite as: J. Chem. Phys. 155, 214301 (2021); doi: 10.1063/5.0066626
Submitted: 11 August 2021 • Accepted: 8 November 2021 •
Published Online: 1 December 2021

N. C. Pyper,[1] T. C. Naginey,[2] and Colm T. Whelan[3,a)]

AFFILIATIONS

[1] Yusuf Hamied Department of Chemistry, University of Cambridge, Lensfield Road, Cambridge CB2 1EW, United Kingdom
[2] Department of Materials, University of Oxford, Parks Road, Oxford OX13 PH, United Kingdom
[3] Physics Department, Old Dominion University, Norfolk, Virginia 23529, USA

[a)] **Author to whom correspondence should be addressed:** cwhelan@odu.edu

ABSTRACT

Atoms remaining as recognizably distinct constituents of bulk condensed phases can have properties modified from those of the isolated species. Dense helium bubbles at high pressures are a common form of radiation damage degrading the mechanical and electrical properties of host materials. Detailed knowledge is critical for predicting their long term performance. Modifications of the ground and first singlet excited states of confined compressed helium are investigated using an entirely non-empirical theory based on the results of *ab initio* self-consistent field calculations with corrections for the effects of electron correlation. For finite sized portions representing bulk condensed fcc and bcc phases of helium atoms, Hartree–Fock wavefunctions, energies, and charge distributions were computed as a function of different atomic densities using two models. The first model for the first excited state localizes the excitation on the central atom; in the second model, this is partially delocalized over the closest atomic neighbors. Total energies for the finite size portions are derived by adding the inter-atomic dispersive attractions and a density functional description of the short-range inter-atomic correlation energy. The experimental energy of the first allowed electronic transition increases with density being larger than in an isolated atom. The intra-atomic correlation energy does not contribute to this energy shift. The calculated energy shifts agree well with experiment for both bulk solid and liquid helium. The 2p orbital is increasingly compressed by density enhancement, thus generating the energy shifts. Consequently, calculations of the inelastic electron scattering cross sections are substantially incorrect if the compression of the final 1s2p state is not included. The character of the excitations is examined, and it is argued that these are of Frenkel rather than the Wannier type.

I. INTRODUCTION

There are many condensed phases in which individual mononuclear species, either atoms or ions, can be clearly identified. Such phases may be composed of either just a single type of atom or, alternatively, more than one species. The first of these types are bulk assemblies in which each of many atoms is confined by atoms of the same type, as in the condensed phases of the noble gases.[1,2] Ionic solids, the overwhelming majority of which are composed of ions of differing nuclear charges, provide widespread examples of the second type.[3,4] The observation that the individual species are readily identifiable has the consequence that it is meaningful to consider that each atom or ion still has its own individual properties even though these may be significantly modified by its environment. This concept of the individuality of each species is especially strong when this retains the symmetry that it has in the isolated state. However, even when the symmetry is essentially unchanged on entering a condensed phase, other properties of the atoms or ions may be very significantly modified. Examples are single species properties such as those of a guest atom trapped in a cage of zeolites[5] in α-quartz[6] and in a noble gas matrix[7] and enclosed in a fullerene molecule,[8] as well as charge distributions and polarizabilities of ions in crystals. Furthermore, quantities involving pairs of species such as the short-range repulsions between ions in crystals and the van der Waals coefficients determining their dispersive attractions can be significantly modified by their condensed phase environments.

Experimental measurements of the properties of condensed phases naturally yield values for the entire bulk system. This has the consequence, certainly in heteroatomic systems, that theory combined with accurate calculations is needed to deduce the properties of the individual species. Such theories can be divided into those in which a single species is taken to interact with a simple model potential description of the environment, as opposed to more accurate and sophisticated treatments involving explicitly the wavefunctions of neighboring atoms or ions.

The simplest model for a condensed phase environment takes the mononuclear species to be enclosed in a spherical shell of radius R_s centered on a nucleus with the potential energy being infinite at all distances from the nucleus greater than R_s. This model has provided insights into the modifications of the energies of both ground and excited states of simple atoms[9–12] as well as in the modifications of the energy ordering of transition metal configurations having different numbers of $(n-1)d$ and ns electrons but fixed total numbers of such electrons.[8,13] The overall conclusions were not only that the confinement raises the energies of all the orbitals, but also, more significantly, that their energy orderings tend to being primarily determined by the n quantum number with the energies for fixed n decreasing with increasing angular momentum. Some attention has been focused on the R_s values at which the binding energy vanishes so that the electron is confined solely by the wall. It has been suggested[14] that the consideration of such states might yield useful insights into transition states and chemical reactivity. Although the infinite potential box model has yielded valuable insights, it has been long recognized that it very significantly overemphasizes the energy shifts predicted using plausible values of R_s. This motivated the various modifications in all of which the infinite potential is softened. The studies[8,13] of confinement induced modifications of atomic orbital energies were extended[15] using the polarizable continuum modification that retains a sphere of radius R_s but is augmented with a continuum model of the material beyond R_s. These energy modifications have also been studied[16] by using the spherical soft confinement potential of the form $(\frac{r}{r_0})^N$, where r is the distance of the electron from a nucleus and r_0 and N are adjustable constants. In the padded box model, the infinite potential is replaced by a constant finite value $[v_0(R_s)]$ with a subsequent modification, the Δ model, restricting this potential to a fixed range (Δ) of distance. Useful insights were afforded by the former in studying[17] a hydrogen atom trapped in either α-quartz or a noble gas matrix or ground state helium[18] and by the Δ model[8] in examining an atom trapped in a fullerene and its photoionization.[13] However, since there would appear to be no *a priori* method for determining the values of any of the parameters $r_0, N, R_s, v_0(R_s)$, or Δ, any comparisons between theory and experiment are at best only semi-quantitative.

The more sophisticated descriptions of the environment needed to obtain results more accurate than those afforded using the model potentials require introducing the wavefunctions of neighboring atoms or ions. These can be implemented in at least two different ways. In the first, a finite sized portion of the bulk material is investigated by using *ab initio* electronic structure computations.[19] In the second, the wavefunction of a central atom or ion is determined through a variational energy minimizing process in which the wavefunctions of neighboring species are explicitly introduced.[3] For any one single ion or single pair of ions, the literature for many years contained a wide range of values for both its polarizability and van der Waals coefficients because simple model potential descriptions of the environment proved to be inadequate. This situation was only resolved by examining a small portion of each ionic lattice through *ab initio* electronic structure computations.[19–23] Similarly, the charge distributions of ions in crystals as well as the cohesive properties of ionic crystals were only moderately well described using simple models for the environment. Fully satisfactory descriptions[3,24] of the anion charge distributions in-crystal have been provided by *ab initio* methods, while good descriptions of the cohesive properties of ionic solids are provided by the second *ab initio* approach.[3,24] The wavefunctions of neighboring cations appear explicitly in both these *ab initio* methods.

The influences of confinement on noble gases, especially helium, have been extensively investigated using both the model potentials discussed above and more sophisticated approaches.[25–27] Furthermore, it is well established experimentally that the energy of the $1s^2 \rightarrow 1s2p(^1P)$ transition in helium is shifted to higher energies in both the bulk liquid and solid phases[2,28–31] as well as in bubbles of helium trapped inside metallic matrices.[32–37] Since model environmental potentials with their adjustable parameters would be inadequate for developing a quantitative theory of these energy shifts, it is necessary to use a more sophisticated theory in which the wavefunctions of atoms neighboring the atom primarily excited are introduced. Thus, the *ab initio* electronic structure computations of a finite portion of the bulk used to study ion polarizabilities are ideally suited to the investigation of excitation energy shifts in helium. The explicit appearance of the wavefunctions of the neighboring atoms, namely, in this case helium, is clearly conceptually different from the alternative introduction of helium atoms as a generic model for the effects of overlap on a species of primary interest. This latter approach has been used[38] to gain insights into the in-crystal modifications of the polarizabilities the group IIB ions as well as the behavior of trapped electrides.[39]

For the bulk condensed phases, the energy of the transition has been measured over a wide range of accurately known pressures, varying from ambient conditions[28] to highly compressed materials.[2,30,31] Experimentally, it was found that the energy of this transition increased with pressure, thus raising the possibility that the measurement of the enhancement (ΔE) of this energy above that in the free atom could be used to determine the density of helium encapsulated as bubbles in other materials. This transition energy was indeed found to be enhanced in the bubbles where the densities and hence the pressures are not reliably known. Such bubbles are technologically significant because they occur during ion implantation in Si[34,40] and in nuclear waste disposal[41] and readily form in the metallic cladding of nuclear reactors.[32,42] The helium densities in bubbles determine the pressures acting on the confining matrix, which pressures may, if greatly elevated, negatively impact the structural integrity of the host material. Nanobubbles embedded in different materials[32,34–37] have also been studied by electron energy-loss spectroscopy (EELS) using a Scanning Transmission Electron Microscope (STEM). Such studies allow electronic excitations to be explored at high spatial resolution, and it has been suggested[36] that the EELS measurement of the energy shift could be used to determine the density and hence deduce the pressure exerted on the bounding atomic matrix. However, the scattering

amplitude of an atom in the bubble was taken to be the same as that of the free atom, which assumption has been shown to be at best dubious.[27] Furthermore, the energy shifts measured for bubbles in different hosts varied widely in non-systematic ways.

The object of this paper is to investigate the nature of the $1s^2$ to $1s2p(^1P)$ excitation with particular emphasis on the excited state. Thus, it will be determined, in the event that the excitation is of the Frenkel type largely localized on the atom, how significantly the energy shifts (ΔE) and 2p electron charge distributions differ in fcc or bcc structured bulk solid phases. The influence of these different environments on the primary variables determining the scattering amplitudes in the EELS experiments will also be elucidated. Furthermore, the predictions derived assuming that the excitation is of the much more delocalized Wannier type will be compared with those yielded by the computations based on the Frenkel description with the aim of elucidating the nature of the $1s2p(^1P)$ excited state.

II. THEORY AND METHODS

A. Overview

The effect of bulk condensed phase environments on the $1s^2$ to $1s2p(^1P)$ excitation energy is investigated by taking the atom primarily excited to be located at the center of a finite sized portion of the bulk and computing the electronic structure of both its ground and excited states.

Each portion of either a bcc or fcc structured lattice is taken to be sufficiently large that both the central atom and its close neighbors experience the environment of an atom in the bulk. Hence, all the closest inter-atomic separations are identical. This contrasts with finite sized clusters of atoms in the gas phase, objects of interest in their own right (see, e.g., Ref. 43), in which the closet inter-atomic separations are not constant. The bcc structure is considered because there is evidence[42,44] that, for the liquid at ambient pressures, each atom is eightfold coordinated with a local structure approximating to bcc. Furthermore, it has been reported[44] that this structure is adopted by one of the phases observed for the bulk solid. The fcc structure is examined since this is adopted by solid helium at the highest temperature and pressures,[46,47] with an hcp phase occurring at slightly lower pressures. In the fcc and bcc structures, the closest inter-nuclear separation R is related to the density n of atoms per unit volume through

$$R = \begin{cases} \left(\frac{\sqrt{(2)}}{n}\right)^{\frac{1}{3}} & \text{fcc}, \\ \left(\frac{3\sqrt{3}}{4n}\right)^{\frac{1}{3}} & \text{bcc}. \end{cases} \tag{1}$$

For a lattice portion with inter-atomic separation R, the $1s^2$ to $1s2p(^1P)$ excitation energy denoted by $\Delta U(R)$ is given by

$$\Delta U(R) = U_e(R) - U_g(R). \tag{2}$$

Here, $U_g(R)$ is the energy of the lattice portion in which all the atoms are in their ground states, while $U_e(R)$ is that of the lowest energy excited state of the lattice portion accessible from the ground state by an allowed transition. The shift $\Delta E(R)$ of the excitation energy from that of the $1s^2$ to $1s2p(^1P)$ transition in a free helium atom is thus given by

$$\Delta E(R) = \Delta U(R) - \Delta U(\infty). \tag{3}$$

Each of the energies in (2) can be expressed as the sum of the contribution predicted in an orbital model, which is expected to be close to the full Hartree–Fock result, plus a remaining minority contribution arising from electron correlation. The *ab initio* computations of the near Hartree–Fock contributions generate the electron wavefunctions used to compute both the scattering cross sections to be discussed in detail elsewhere, as well as one of the electron correlation contributions to $\Delta E(R)$. Furthermore, the resulting near Hartree–Fock wavefunctions yield the moments of the spatial distribution of the excited electron. These provide physical insights into the environmentally induced modification of the orbital that reduces to the pure $2p$ function of the free atom.

B. The near Hartree–Fock computations

1. Wavefunction generation

In the electronic ground state of a lattice portion, each helium atom was described by its free atom $1s^2$ Hartree–Fock wavefunction since these two electrons are sufficiently tightly bound that their wavefunctions will remain essentially unchanged on entering a condensed phase. This description is supported by the evidence presented in Appendix A. Two different models of the electronic structure of the excited lattice portion were considered, these being called basic and extended.

In the basic model, the excitation is taken to be essentially localized on the central atom. Thus, the only atomic orbital of the p symmetry is located on this atom with this orbital being fully optimized to take account of its modification caused by its condensed phase environment. The single 1s electron on the central atom was taken to occupy the 1s orbital of the He^+ ion because the optimal (i.e., exact Hartree–Fock) 1s orbital in the free atom $1s2p(^1P)$ state was shown[26] to be identical to this orbital in the cation. Each of the remaining atoms in the excited state of the lattice portion was described by the free atom $1s^2$ Hartree–Fock wavefunction as described for the ground state. This approach is supported both by the arguments presented below in the description of the extended model and by the analysis in Appendix A.

The extended model allows for the possibility of the excited electron becoming partially delocalized into the $2p$ orbitals on the closest atomic neighbors of the central atom. Hence, the same primitive basis set of Gaussians, which is located on the central atom in the basic model, is also placed on each of these neighbors. The final excited state orbital emerges from the Hartree–Fock computation. The 1s orbital in the 1s2p excited state is even more contracted than that in the $1s^2$ ground level. In the extended model, some of the excited charge is transferred to the closest neighbors, which suggests that some of the 1s electron density on these atoms could be transferred back to the central atom to retain local charge neutrality. This possibility is accommodated by introducing two specially constructed contracted 1s basis functions on both the central atom and each of its neighbors, the details being presented in Appendix A.

Each remaining atom, not carrying any p symmetry basis functions, is described using the Hartree–Fock orbitals of the free atom ground state as already described.

A significant technicality of the computations for the excited state is discussed in Appendix B. It is shown that it is necessary to ensure that the orbital containing the excited electron has a symmetry that is consistent with that of the lattice portion.

2. Determination of the sizes of the lattice portions

The helium $2p$ orbital is sufficiently weakly bound that, in this excited state in a condensed phase, it has a non-negligible probability density in spatial regions outside the first coordination shell. This means that, for a bulk condensed phase or an atom in the center of a bubble, the results of computations of the properties of the 1s2p state are only trustworthy if the number of coordinating shells of neighbors is sufficiently large that the predictions remain unchanged on introducing a further shell of atoms. The results presented in Table I for two representative densities of the bcc structure, computed in the extended model, show how moments of the $2p$ electron density and near Hartree–Fock predictions of the excitation energy converge with increasing lattice portion size. In Table I, N_S and N_C are the number of coordinating shells and the number of atoms, respectively, including the central one.

The results in Table I illustrate the observation[26] that computations introducing only the first coordination shell predict that the $2p$ orbital can, in some cases, be greatly expanded compared with that in the free atom. Thus, for example, the results in the first line show that, at low densities, the introduction of just a single shell yields a $2p$ orbital that is significantly contracted compared with the corresponding free atom r^2 and r^4 values of 31.55 and 1831a.u. However, at higher densities such as 0.05 atoms Å^{-3} considered in the lower half of Table I, the use of just a single shell of atoms is insufficient to capture the $2p$ orbital compression occurring in the bulk as this calculation predicts a spurious vast expansion of the $2p$ orbital. However, the results for all the lattice portions with more coordinating shells show that this prediction of expansion produced by the one shell model is erroneous. Thus, even the introduction of the second shell predicts that the $2p$ orbital is actually very significantly contracted compared with that in the free atom. This contraction arises[26] from the energy increase originating ultimately from the Pauli principle when the 2p orbital overlaps with the filled 1s orbitals of neighboring unexcited atoms. The erroneous prediction of orbital expansion in the one shell model arises from the absence of this repulsion at distances beyond that of the first shell. Furthermore, these results show that the prediction of the energy shift is fully converged for comparison with experiment after the introduction of the third shell of neighbors. Thus, the previously reported[26] results for the energy shifts did not suffer from lack of convergence. Computations of energies based on the variation principle, as for the present near Hartree–Fock results, should be expected to have smaller errors than the predictions of properties derived from such wavefunctions. Thus, even though the computations including only one coordinating shell can erroneously predict large orbital expansions, the energy shifts emerging from such calculations are not at all unreasonable. The results for the second and fourth moments of the $2p$ electron density show that these predictions require the introduction of more coordinating shells than needed for accurate predictions for the energy shifts. Furthermore, as would be expected, more shells are required for properties having greater contributions from a larger distance from the position of the $1s2p$ excited atom. Thus, even the results for $\langle r^2 \rangle$ are not fully converged after introducing just three neighboring shells. Nevertheless, the results of Ref. 26 were sufficiently accurate as to serve their purpose of understanding the nature and reasons for the influence of the environment on the behavior of the $2p$ orbital. In contrast, the previously reported results for $\langle r^4 \rangle$ were not converged even though these predictions decrease on increasing the number of coordinating shells.

TABLE I. Convergence of property predictions with increasing lattice portion size. Here n is the number of atoms per Å^{-3}, the moments and energies are in a.u. For n values of 0.0286 and 0.05, R = 6.9361 and 5.7577 a.u., respectively.

n	N_S	N_C	$\Delta U^{SCF}(R)$	$\langle r^2 \rangle$	$\langle r^4 \rangle$
0.0286	2	15	0.6853	19.66	717.20
0.0286	4	51	0.6944	18.62	572.14
0.0286	5	59	0.6944	18.62	572.40
0.0286	6	65	0.6944	18.61	570.90
0.05	2	15	1.6024	147.54	30 650.5
0.05	4	51	1.6501	14.29	358.50
0.05	5	59	1.6498	14.22	336.72
0.05	6	65	1.6496	14.21	334.82

C. Electron correlation contributions

1. Overview

Electron correlation in the helium atom lattice portions consists of a sum of intra-atomic and inter-atomic contributions. The former consists of the electron correlation contribution to the energy of a single atom having the wavefunction optimal for its condensed phase environment. The inter-atomic correlation energy is that entering the expression for the energy of interaction of two or more atoms.

2. The intra-atomic correlation energy

The intra-atomic correlation energy of a single atom in the $1s2p(^1P)$ excited state is negligibly small. The intra-atomic correlation energy of the free atom $1s^2$ ground state is around 1 eV, thus making a non-negligible contribution to the $1s^2$ to $1s2p(^1P)$ excitation energy $\Delta U(R)$, this being 21.22 eV in the free atom. However, the environmental insensitivity of the contracted ground state will cause this correlation energy contribution to be essentially independent of density. Consequently, this energy does not contribute to the excitation energy shift $\Delta E(R)$ evaluated from (3). This result coupled with the essential vanishing of the intra-atomic contribution to the correlation energy of a $1s2p$ excited atom shows that intra-atomic correlation energies do not contribute to the energy shift. Full details of these correlation contributions are presented in Appendix C.

3. The inter-atomic correlation energy

The inter-atomic correlation energy in the lattice portions can be decomposed into the sum of contributions of short and long

ranges.[47] The former arises from the overlap of the electron densities of the interacting atoms, while the latter constitutes the dispersion energy. The dominant contributions to both these correlation energies arise as the pairwise sum of the interactions between pairs of atoms. The short-range correlation contribution to the interaction between each pair of atoms was calculated by assuming that the pair electron density could be described as a superposition of the atomic densities as used in the density functional description of a uniform electron-gas, the Gordon–Kim approach.[48] There is good evidence, presented in Appendix C, that the addition to the dispersion energy of the short-range correlation energy thus calculated does not introduce any significant double counting of correlation effects. The basic expression for the long range inter-atomic correlation energy, constituting the dispersive attraction, is derived by perturbation theory neglecting the exchange of electrons between the interacting atoms. This can be rearranged into the standard multipolar expansion for inter-atomic distances sufficiently large that the electron densities of the interacting atoms do not overlap. However, for shorter distances where overlap is appreciable, each term in the multipolar expansion is modified by multiplication by a well-defined damping factor.[49] The dispersive attraction between each pair of atoms was derived using the dipole–dipole dispersion coefficients and parameters determining the damping of the attractions at short distances, as outlined in Appendix C.

III. RESULTS

A. Excitation energies and electron charge distributions

1. Density dependence of the excitation energies

The energy shifts measured for the bulk material as a function of density are compared in Table II with those predicted using both the basic and extended models for both the bcc and fcc structures. The calculated results include all three (near Hartree–Fock, short-range correlation, and dispersion) contributions to $\Delta E(R)$.

The calculation in the first row of Table II used a model for the bulk liquid at its experimentally determined density experiencing only its own very small vapor pressure (about 1 mmHg) at the very low temperature of 1.4° K. The excited atom was taken to be located at the center of the bcc lattice with just two shells of neighbors. This description is appropriate because scattering experiments, with first neutrons[50] and subsequently x rays,[51] showed that there are only two clearly defined coordinating shells. Perfect agreement with the early experiment of Ref. 28 is achieved. All the results in Table II, excepting those in the first row, were performed for both the fcc and bcc structures using the five shells of atoms needed to produce fully converged predictions as shown by the data in Table I. This is the description needed for comparison with the experimental results for the bulk liquid and solid phases at high pressures where the atomic mobilities will be significantly restricted. At the time of our first calculations in 2001,[26] there were only two measurements of the energy shift in bulk helium, that of Refs. 28 and 29 the latter having very significant error bars. However, our extended model predictions (Table II) for the shifts show excellent agreement with the significantly more accurate $\Delta E(R)$ measurements[2,31] subsequently presented for a range of directly experimentally determined pressures. This agreement, when compared with the overestimation of $\Delta E(R)$ by the basic model, shows that the excitation is partially delocalized onto neighboring atoms.

In the experiments of Refs. 2, 30, and 31, the liquid helium sample was contained in a high pressure system at a known temperature and pressure.[52] The corresponding molar volumes were determined from existing PVT measurements[53] and the energy shift measured. It is a straightforward matter to deduce the density from the molar volume. It is to be stressed that all relevant quantities were either measured or deduced from well-established measurements, and there was no extrapolation of either experimental or theoretical data. Furthermore, in the experiment[31] on the solid, the unit cell parameters were determined by x-ray diffraction, thereby yielding an accurate value for the density. Consequently, these experiments provide an accurate and entirely trustworthy set of data to compare

TABLE II. Calculated and experimental total energy shifts: (1) Two-shell model for bulk liquid, (2) bulk liquid at low ambient pressure, (3) one Gaussian fit (as defined in Ref. 2), and (4) excitation energy as given in Ref. 2 citing previously unpublished material from Ref. 30.

	$\Delta E(R)$ cal				$\Delta E(R)$exp	
Atoms Å^{-3}	bcc (basic)	fcc (basic)	bcc (extended)	fcc (extended)	Energy	Ref.
0.022	0.377(1)	⋯	⋯	⋯	0.38 ± 0.06	28(2)
0.0286	0.599	0.605	0.506	0.496	⋯	⋯
0.04	1.028	1.032	0.881	0.856	⋯	⋯
0.0419	1.101	1.106	0.945	0.919	0.88	2(3)
0.0446	1.205	1.211	1.036	1.006	0.68 ± 0.3	29
0.045	1.220	1.226	1.050	1.018	⋯	
0.0460	1.259	1.266	1.084	1.052	1.02	2(3)
0.0492	1.384	1.390	1.192	1.157	1.115	2(3)
0.05	1.415	1.420	1.219	1.182	⋯	⋯
0.0518	1.484	1.492	1.279	1.242	1.31	2(3)
0.0536	1.554	1.562	1.340	1.301	1.35	2(4)
0.0562	1.654	1.663	1.427	1.384	1.38	31

with our theoretical predictions. It is to be stressed here that neither our theory nor the experiments are in anyway adjusted. The excellent agreement between the completely reliable experimental measurements and our calculations encourages our confidence in the soundness of our *ab initio* approach. The essential point is that one has experimentally measured values of the energy shift as a function of experimental determined densities (i.e., R) any pressure values being merely incidental, just being used to obtain the density.

The results in Table II show that, for the same density, the shifts predicted for the bcc and fcc structures are essentially identical. This shows that the previous agreement[26] between experiment and the calculations made for the fcc structure did not rely on the assumption that the experimental measurements were made for a bulk material having this particular structure.

2. The 2p electron charge distribution

The results in Table III show that the second and fourth moments of the 2p electron charge distributions predicted for the fcc and bcc structures differ only minutely, thus being consistent with the similarities of the predicted energy shifts. Furthermore, these charge distributions become increasingly contracted at higher atomic densities. An explanation of the physics underlying both the 2p orbital contractions and the positive energy shifts was proposed in Ref. 26. It was argued that, if the atom, which is ultimately excited, is a member of a lattice portion where the atomic separations are sufficiently small, the 2p orbital on the central atom would overlap the electron densities of the surrounding atoms. The Pauli principle requires that the wavefunction describing all the electrons in the system should be anti-symmetrized. When the 2p orbital is orthogonalized to the 1s orbitals on the surrounding atoms, extra nodes are introduced into the 2p orbital, which increases its energy. The energy of the lattice portion can be reduced by using a more contracted 2p orbital, but this energy is still greater than before the Pauli principle was taken into account. This compression of excited helium precisely mirrors the contraction of the wavefunction and reduction in the polarizability of an anion on passing from the free state into a bulk ionic crystal.[3,21]

The closest inter-atomic separation (R) in a bcc crystal is smaller than that in an fcc crystal having the same density as the latter is a close packed structure in contrast to the former. The smaller R value in the bcc crystal will act in the direction of producing a 2p orbital more contracted than that in the fcc material having the same density. However, an atom in the fcc material has a larger number (12) of closest neighbors than an eightfold coordinated atom in the bcc structure. Consequently, the 2p orbital in the fcc structure will experience a greater compressive effect than one in the bcc material having the same value of R. This effect acts in the opposite direction to the smaller R value in a bcc material having the same density as an fcc crystal. The net result of these two competing effects produces nearly identical energy shifts and 2p electron charge distributions in the fcc and bcc materials.

TABLE III. Computed spatial moments of the 2p electron charge distribution. Here n is the number of atoms per Å^{-3}, the moments are in a.u. For all non-zero densities, we have 5 shells with 59 atoms in the bcc case and 79 atoms for fcc.

	Basic model				Extended model			
	$\langle r^2 \rangle$		$\langle r^4 \rangle$		$\langle r^2 \rangle$		$\langle r^4 \rangle$	
n	bcc	fcc	bcc	fcc	bcc	fcc	bcc	fcc
0.0	31.6	31.6	1831	1831	...	...	...	...
0.0286	17.4	17.3	472	469	18.6	19.0	572	589
0.04	14.6	14.5	333	328	15.8	16.3	412	432
0.045	13.7	13.6	297	290	15.0	15.4	368	388
0.05	12.9	12.9	272	262	14.2	14.6	337	352
0.0562	12.2	12.1	254	239	13.5	13.9	327	319

3. Comparative overview of the liquid and three solid phases

The agreement between predicted (Table II) and measured energy shifts is equally good for the solid material[31] as for the liquids under high pressures.[2] This is entirely consistent with the experimental result that there is very little difference between the shifts exhibited by the liquid and solid materials provided that these have very similar densities. This result adds credence to the use of our model for the liquid at high pressures.

In the hcp and fcc structures, not only does each atom have the same number of closest neighbors, but, furthermore, the closest neighbor distances (R) are identical in materials having the same density (n). Consequently, the difference in the atomic environments in fcc and hcp crystals having the same density will be very much less than that between the fcc and bcc atomic environments. This observation, coupled with the result that the fcc and bcc materials of the same density have similar 2p orbitals and energy shifts, provides strong evidence that these properties will be virtually identical in fcc and hcp materials of the same density. This shows that our calculations for an fcc structured material and the experimental results[29,31] for the hcp crystals are fully comparable so that the good agreement between theory and experiment did not arise from examining the fcc structure. The measured[46,47] very small entropy and volume changes of the phase transition from the hcp to the fcc structure is a further indication of the close similarities of these two materials.

B. The Wannier excitation model

1. Theory and implementation of the Wannier model

The previous calculations yielded 2p orbitals that are quite localized in that they do not significantly extend beyond the second coordination shell of the atom primarily carrying the 2p excitation, thus being of the Frenkel type. The excitation spectrum of helium has also been measured[54] at pressures much higher than those in the experiments referenced in Sec. III A with the temperature of 300° K also being significantly higher than those around 10–20° K in the studies.[2,28,31] It was suggested[54] that these excitations could be of the Wannier type, the essence of these differing considerably from the approach used in our computations. This suggestion provides one motivation for examining the possibility that the $1s^2$ to $1s2p$ excitations in the experiments[2,28,31] are Wannier in character. Furthermore, possible differences between the Wannier wavefunctions and those predicted by the present computations can affect the scattering amplitudes discussed in Sec. III C.

In the Wannier model, the potential energy of the excited p electron is taken, in atomic units, to be

$$-\frac{1}{\varepsilon(n)r}.$$

Here, r is the distance of the electron from the nucleus of the $1s^1$ He^+ core resulting from the excitation and $\varepsilon(n)$ is the density dependent dielectric constant of the unexcited bulk medium. This interaction energy can be taken to constitute the entire potential energy relative to any given binding energy of a free electron in bulk helium. The large spatial extent expected for wavefunctions of the Wannier type justifies both neglecting its penetration into the ion core and introducing the bulk dielectric constant. The introduction of an effective mass m^* for the $2p$ electron yields the energy $e_{2p}(n)$ and mean square radius[55] of the resulting hydrogen like system as

$$e_{2p}(n) = -\frac{m^*}{8[\varepsilon(n)]^2} \tag{4}$$

and

$$\langle r^2 \rangle = 30\left[\frac{\varepsilon(n)}{m^*}\right]^2, \tag{5}$$

where all quantities are expressed in a.u. The validity of the assumption that, in the $1s2p$ excited state, the penetration of the p electron into the $1s^1$ core can be neglected is supported by the result that properties of the $2p$ orbital in the free atom are closely reproduced by the Wannier description with ε and m^* taken to be unity. Thus, the binding energy $e_{2p}(0)$ of −3.401 a.u. predicted from (4) agrees closely with the −3.496 eV average (see Appendix D) of the experimental binding energies of the $1s2p(^3P)$ and $1s2p(^1P)$ levels relative to the ionized $1s^1$ He^+ ground state. Furthermore, Table IV shows that the 30 a.u. prediction from (5) of $\langle r^2 \rangle$ is very similar to the Hartree–Fock result of 31.55 a.u.[56] for the $2p$ orbital in the $1s2p(^1P)$ level of the free atom.

The application of the Wannier model predicts that the energy shifts, $\Delta E_W(n)$, are given by

$$\Delta E_W(n) = e_{2p}(n) - e_{2p}(0). \tag{6}$$

The Wannier model can only reproduce the average of the binding energies in the $1s2p(^3P)$ and $1s2p(^1P)$ states because this description does not include the exchange interaction between the $2p$ and the 1s electrons. The discussion presented in Appendix D shows that $e_{2p}(0)$ in (6) should be taken to be −3.401 a.u., which is the Wannier prediction for the isolated atom binding energy. The dielectric constant at each density was derived by using the standard Clausius–Mossotti equation, as described in Appendix D. The important qualitative point is that $\varepsilon(n)$ increases with increasing density.

2. Comparison of Wannier model, ab initio computations, and experiment

The results presented in Table IV compare the energy shifts predicted using the Wannier model having $m^* = 1$ with those of our computations. The latter are the totals, being the sum of the self-consistent field (SCF), short-range correlation, and dispersion contributions. The Wannier predictions are independent of the structure being the same for the bcc and fcc systems. The energy shifts predicted from the exciton model for small n are not that dissimilar to those of our computations. However, they deviate significantly from both the computations and experiment as the number density increases.

Although both the Wannier description and our calculations agree in predicting that the shift increases with density, these predictions arise for completely opposite reasons. Thus, the Wannier model predicts larger shifts with an increase in n because the electron becomes more loosely bound on account of the increase in $\varepsilon(n)$ with density, this being expressed in the mathematics by the $[\varepsilon(n)]^2$ factor in the denominator of (4). It then follows from (5) that $\langle r^2 \rangle$ of the Wannier orbital increases with increasing density. By contrast, our computations predict that the $2p$ electron becomes more tightly bound as measured by its energy because it becomes increasingly compressed by its overlap with the filled 1s orbitals on neighboring atoms. This effect is not included in the Wannier model. The representative results assembled in Table IV confirm the opposite dependencies of $\langle r^2 \rangle$ predicted by the Wannier and *ab initio* descriptions.

A value for the effective mass m^* could be determined by demanding that (6) reproduces the experimentally observed $\Delta E(R)$. These masses are deduced by rearranging (6) and substituting the

TABLE IV. Wannier model predictions for energy shifts and mean square radii. Densities n are in atoms Å^{-3}, and energy shifts are in eV with other quantities being in a.u.

		Energy shifts (eV)[a]			Fitted	Wan$\langle r^2 \rangle$		b
n	$\varepsilon(n)$	$\Delta E_W(n)$	$\Delta E^0(R)$	$\Delta E(R)$	m^*	$m^* = 1$	Fit m^*	$\langle r^2 \rangle$
0.0	1.0					30.0		31.5
0.0286	1.076	0.463	0.605	0.496	0.989	34.7	35.5	19.0
0.04	1.107	0.625	1.032	0.856	0.917	36.8	43.7	16.3
0.045	1.121	0.694	1.226	1.018	0.880	37.7	48.7	15.4
0.05	1.135	0.761	1.420	1.182	0.840	38.6	54.8	14.6

[a] $\Delta E^0(R)$ and $\Delta E(R)$ from the present basic and extended computations for the fcc structure.
[b] *Ab initio* calculations using the fcc structure with the extended model.

observed $\Delta E(R)$ on the left-hand side. This yields m^* in a.u. with $e_{2p}(0)(=-3.401)$ and $\Delta E(R)$ in eV,

$$m^* = 8[\varepsilon(n)]^2 \frac{[-e_{2p}(0) - \Delta E(R)]}{27.2116}. \quad (7)$$

Since $\Delta E_W(n)$ is always less than the value predicted when m^* is taken to be unity, it follows from (7) that the m^* values must become increasingly smaller with an increase in n if $\Delta E(R)$ is to be reproduced. These reductions in m^* produce larger values (Table IV) of $\langle r^2 \rangle$ than those derived taking m^* to be one. Thus, the introduction of empirically determined m^* values merely accentuates the differences between the Wannier and *ab initio* mean square radii.

3. Inapplicability of the Wannier description

The Wannier model predicts that more extended orbitals arise for the systems with the larger $\varepsilon(n)$. For $n = 0.05$ with an $\varepsilon(n)$ value of 1.140, the fitted m^* predicts a mean radius $\langle r \rangle$ of 6.7 a.u. derived using the result[57]

$$\langle r \rangle = \left(\frac{\varepsilon(n)}{2}\right)\left[\frac{3n_p^2 - l(l+1)}{m^*}\right]. \quad (8)$$

This radius is comparable or smaller than the closest inter-atomic separations considered in either the experiments or the calculations. This shows that it cannot be valid to use the bulk dielectric constant in any treatment of the interaction of the $2p$ wavefunction with its environment. The use of the bulk $\varepsilon(n)$ is only valid if the wavefunction encompasses a very large number of atoms rather than just overlapping with a few nearest neighbors. This analysis of the Wannier model predictions coupled with the results of our near Hartree–Fock plus inter-atomic correlation approach provides all the evidence required to support the suggestion[29] that the $1s^2$ to $1s2p$ excitation is of the localized Frenkel type. This strongly suggests that this excitation does not arise from an interaction of a Wannier excitation with an interband transition as suggested later.[54] However, this comment may not extend to their reported higher energy excitations as the helium densities examined[54] were about three times larger than those considered here. The Wannier model is only applicable to hosts, such as semi-conductors having $\varepsilon(n)$ values of the order of 10 when the resulting mean radius of about 50 a.u. ensures that the wavefunction encompasses at least hundreds of atoms. This consideration, coupled with the increasing discrepancies between $\Delta E_W(n)$ and $\Delta E(R)$ with increasing n (decreasing R), shows that the Wannier model does not correctly describe the helium $1s2p$ excited state.

C. Condensed phase modifications of inelastic electron scattering

It is technologically important to be able to determine accurately the pressures exerted by helium bubbles formed in the walls of nuclear reactors.[35,42] However, these pressures cannot be measured directly and have to be deduced from a trustworthy equation of state for helium at high pressures, the use of such equations requiring knowledge of the helium density. It has been suggested[36] that this latter could be derived by directly measuring the radius of a bubble by using electron microscopy while deducing the total number of atoms in the bubble from inelastic electron scattering experiments in which ground state atoms are excited to the $1s2p(^1P)$ level. It was assumed, in this procedure, that the inelastic scattering cross section in the bubble was the same as that for a free helium atom.

The inelastic scattering cross section, σ, is given by[59,60]

$$\sigma = \frac{4\pi}{E_i}\int_{q_{min}}^{q_{max}} \frac{|\varepsilon_{2p}(q)|^2}{q^3} dq, \quad (9)$$

where E_i is the energy of the incident electron and q_{min} and q_{max} are the magnitudes of the minimum and maximum values of the momentum transfer q. $\varepsilon_{2p}(q)$ is the atomic form factor given by

$$\varepsilon_{2p}(q) = \langle \Psi_g(\mathbf{r}_1, \mathbf{r}_2) | \sum_{j=1}^{2} e^{i\mathbf{q}\cdot\mathbf{r}_j} | \Psi_e(\mathbf{r}_1, \mathbf{r}_2) \rangle. \quad (10)$$

Expressing both the ground $|\Psi_g(\mathbf{r}_1, \mathbf{r}_2)\rangle$ and excited state $|\Psi_e(\mathbf{r}_1, \mathbf{r}_2)\rangle$ wavefunctions using an orbital description yields

$$\varepsilon_{2p}(q) = \sqrt{2}\langle \psi_{1s}^g(\mathbf{r}) | \psi_{1s}^e(\mathbf{r}) \rangle \langle \psi_{1s}^g(\mathbf{r}) | e^{i\mathbf{q}\cdot\mathbf{r}} | \psi_{2p}(\mathbf{r}) \rangle. \quad (11)$$

Here, $\psi_{1s}^g(\mathbf{r})$ and $\psi_{1s}^e(\mathbf{r})$ are the Hartree–Fock 1s orbitals of the ground and excited states, respectively, while $\psi_{2p}(\mathbf{r})$ is the Hartree–Fock orbital of the $1s2p(^1P)$ excited state. Note that $\varepsilon_{2p}(q)$ is a function of the magnitude of $\mathbf{q}$ only; this is a consequence of

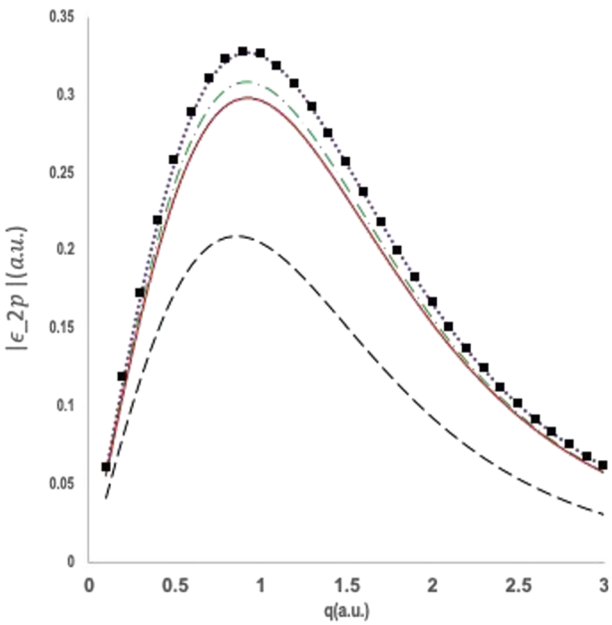

FIG. 1. Atomic form factor for a density of 0.05 atoms/Å^3. Free atom (dashed black), fcc extended (solid red), fcc basic (solid rectangles), bcc basic (purple dotted), and bcc extended (green dashed-dotted) are shown.

the fact that $\langle \psi_{1s}^{g}(\mathbf{r})|e^{i\mathbf{q}\cdot\mathbf{r}}|\psi_{2p}(\mathbf{r})\rangle$ corresponds to an integral over all $\mathbf{r}$; without the loss of generality, we can chose the z direction to be in the same direction as $\mathbf{q}$ and then $e^{i\mathbf{qr}}$ is simply $e^{iqr\cos\theta}$, and we integrate over θ and ϕ. Explicit computations of the overlap integral $\langle \psi_{1s}^{g}(\mathbf{r})|\psi_{1s}^{e}(\mathbf{r})\rangle$ yield a value very close to unity. It is clear that the major contributions to $\langle \psi_{1s}^{g}(\mathbf{r})|e^{i\mathbf{q}\cdot\mathbf{r}}|\psi_{2p}\rangle$ come from small r values where the 1s orbital is appreciable. This strongly suggests that the compression of the $2p$ orbital on entering a condensed phase, demonstrated by the results in Table III, would cause $|\varepsilon_{2p}(q)|$ to be significantly enhanced over that of the free atom.

In Fig. 1, we show $|\varepsilon_{2p}(q)|$, at a density of 0.05 atoms/Å^3, for all four compressed models. Although there are only relatively small differences between the form factors calculated in these models, there are marked enhancements over the free atom calculations. It then follows immediately from (9) that the inelastic scattering cross section in the condensed phase is significantly larger than that of the free atom. This strongly indicates that bubble densities, deduced taking the scattering cross section to be that of a free atom, cannot be trusted. This topic will be discussed more fully elsewhere.

IV. CONCLUSIONS

We have presented a non-empirical approach to the calculation of the atomic properties of confined and compressed helium. The near perfect accord we have achieved with reliable bulk measurements is in contrast to earlier semi-analytic model calculations. In bulk helium under pressures sufficiently high that it exists as either a very dense liquid or a solid, the $2p$ wavefunction in the first excited state becomes compressed by its environment of the other ground state atoms. Here, this compression has been explicitly manifested by the reduction in the moments of its charge distribution. Furthermore, this wavefunction compression causes its energy to be raised above that in the isolated atom. The excitation energy from the ground state of the bulk to that with essentially one atom excited into its 1s2p state is thereby enhanced [by the shift $\Delta E(R)$] relative to that in a free atom. It has been shown by explicit computation that these orbital compressions and excitation energy enhancements in a helium bulk phase having the bcc structure are almost identical to those in an fcc structured material of the same density. These similarities indicate very strongly that the energy shift in an hcp structured phase will be essentially identical to that in the fcc material. These results show that the excellent agreement between the very reliable experimental measurements of these energies shifts and our predictions for the fcc phase does not support this assumption about the structure.

In the Wannier description of the excited state, the attraction of the 2p electron to the He^+ ion created by its excitation is taken to be purely Coulombic but reduced by the dielectric constant of the bulk unexcited material. For bulk materials of lower density, the energy shifts predicted by this description are not too dissimilar to those yielded by the present computations. This similarity arises because the dielectric constant at these lower densities is close to unity, while the potential energy experienced by the $2p$ electron in the $1s2p(^1P)$ state of the free atom is extremely close to that in a hydrogen atom. Although the Wannier model does produce energy shifts that increase with the density of the account of the accompanying enhancement of the dielectric constant, the predictions become increasingly less than the experimental values as the density increases. This is one indication that the excitations are not of the Wannier type, another being that the $2p$ radii predicted by this model do not extend over a number of atoms sufficiently large as to justify using the bulk dielectric constant. The excellent agreement with experiment achieved by our computations, coupled with the inadequacies of the Wannier model demonstrated here, shows that these excitations are not of the highly spatially extended Wannier type. It can, therefore, be concluded that they are much more localized as predicted by our computations.

The compression of the $2p$ orbital in condensed phase environments, as manifested by reduced moments of its charge distribution, causes the atomic form factor to be enhanced compared with that in the free atom. Consequently, the inelastic scattering cross section will be significantly greater than that of the free atom. This needs to be considered in the interpretation of experiments aiming to deduce the atomic densities of bubbles trapped in metals from measurements of the intensity of the inelastic scattering.

ACKNOWLEDGMENTS

This research was supported by the grant from the Royal Society under the International Exchange Scheme. T.C.N. gratefully acknowledges funding from EPSRC under Grant No. EP/LO15722/1. T.C.N. would also like to thank Professor Martyn Guest for invaluable assistance in getting the GAMESS-UK calculations to run smoothly. N.C.P. and T.C.N. thank Dr. Alex Thom for his help in running some of the GAMESS calculations. All the authors thank Professor P. D. Nellist for very many informative discussions.

AUTHOR DECLARATIONS

Conflict of Interest

No potential conflict of interest was reported by the authors.

DATA AVAILABILITY

The data that support the findings of this study are available from the corresponding author upon reasonable request.

APPENDIX A: HARTREE–FOCK BASIS SETS AND GROUND STATE

1. Basis sets, primitives, and contracted

The near Hartree–Fock computations were performed using the GAMESS-UK program.[60] This correctly handles the singlet spin pairing in the open shell electronic structure of the excited states of the lattice portions for which the wavefunction is a sum of two Slater determinants. Thus, the resulting molecular orbitals of the lattice portion have the correct symmetry properties. Each molecular orbital is expressed, ultimately, as a linear combination of primitive Gaussian basis functions as described previously.[26]

In all the computations for the lattice portion excited states, eight primitive Gaussians of the p symmetry were located on the central atom, these remaining uncontracted. In the extended model computations, the same uncontracted basis was also located on each of the nearest neighbors of the central atom. The optimal combination of these basis functions emerges from the self-consistent field (SCF) procedure.

In all the cases considered, the different basis functions of the s symmetry introduced into the SCF calculations were contractions built from the same set of ten primitive Gaussians. The atoms without p symmetry basis functions were described by just the single contraction producing the 1s Hartree–Fock orbital of the free atom $1s^2$ ground state. The 1s orbital on the central atom in the basic model was similarly described by that combination of the ten primitives yielding the exact 1s orbital of an isolated He^+ ion.

It was explained in Sec. II B 1 that, in the extended model, it is necessary to allow the optimal s symmetry orbitals to emerge from the SCF procedure as any linear combination of the free He^+ $1s$ function and the $1s^2$ free atom Hartree–Fock orbital. Since the 1s orbital in an unexcited atom of $1s^2$ configuration differs from that in the $1s2p(^1P)$ excited state, both the central atom and all those in the first coordination shell each had two contracted s symmetry basis functions. For the central atom, the first of these two s type basis functions is the 1s orbital of He^+ with the second being that part of the ground state $(1s^2)$ Hartree–Fock 1s atomic orbital that is orthogonal to the $1s$ He^+ orbital. The first s basis function on each atom in the first coordination shell was the free atom ground state 1s Hartree–Fock atomic orbital with the second basis function being that part of the He^+ 1s atomic orbital that is orthogonal to the $1s^2$ ground state Hartree–Fock atomic orbital. The presence of these two s type basis functions on each atom allows the wavefunction of the unexcited electrons to be optimal for any partial or full occupation of a p orbital residing on the same atom. The orthogonalizations were introduced to avoid the near linear dependency problems that would arise on introducing both the He^+ $1s$ orbital and the $(1s^2)$ Hartree–Fock orbital.

2. Tests of the contracted descriptions of the s orbitals

a. Wavefunction optimization test

In the extended model, two s symmetry contracted basis functions are placed on both the central atom and those in the first coordination shell. The results from the computations for ground states of the lattice portions allow one to probe the assumption made that atoms having no p symmetry basis functions are well described by using just free atom $1s^2$ Hartree–Fock orbitals. In principle, the helium atom wavefunctions would be expected to contract with decreasing R in order to reduce the Pauli type repulsion originating from the overlap of atomic orbitals of two closed shell systems. The computation of the ground state lattice portion wavefunctions in the extended model introduces this effect since both the central atom and those in the first coordination shell have the He^+ $1s$ wavefunction in the basis as well as the less spatially contracted $1s^2$ Hartree–Fock function. The presence of the first of these two functions can allow the wavefunction to contract compared with that in the free atom ground state. Since this effect is not included in the basic model, its importance can be gauged by comparing the ground state lattice portion energies predicted by the two models. The energy lowerings of the lattice portion ground state on passing from the basic to the extended model are presented in Table V.

The results show that any compression of the helium atom wavefunctions in the ground states of the lattice portion does not need to be considered, thus confirming the view expressed previously.[26]

TABLE V. Extended model ground state lattice portion energy lowerings. $U_g^{SCF}(R)$ and $U_g^{SCF0}(R)$ are the extended and basic model total ground state fcc lattice portion energies with numerical values presented in Table B3 of Ref. 26 where $U_g^{SCF}(R)$ are labeled "with orthogonalization."

n (atoms Å^{-3})	0.04	0.05
$U_g^{SCF}(R) - U_g^{SCF0}(R)$ (eV)	0.0005	0.0014

b. Ground state lattice portion energies and the pair potential

In the computations of the energy shifts $\Delta E(R)$, the wavefunctions of the ground states of the helium atoms were taken to be unaffected by their environments with the energies of the ground state lattice portions being computed using these wavefunctions. The resulting ground state lattice portion energies are slightly greater than the sum of the energies of the corresponding numbers of free ground state atoms because their wavefunctions overlap in the lattice portion, thus generating the Pauli type repulsion discussed in Sec. III A 2.

It is useful to consider a group of 13 helium atoms in which the central helium is coordinated by 12 nearest neighbors, thus generating the smallest fraction of a fcc lattice. The assumption that free helium atom $1s^2$ wavefunctions describe the bulk phases is thus probed by comparing the total energy of the 13 atom group with the sum of all the closest pair repulsions.

There will be 12 nearest neighbor repulsions contributing to the energy of the group of 13 atoms. The interaction energy $\Delta U_{2g}^{SCF}(R)$ of two helium atoms has been computed[61] at the fully optimized Hartree–Fock level as a function of R with the results being presented in Table VI. It should be expected that the sum $(12\Delta U_{2g}^{SCF}(R))$ of these repulsions should be comparable with the difference $(\Delta U_{13g}^{SCF}(R))$ between our computed energy $(U_{13g}^{SCF}(R))$ of the 13 atom group and that of 13 free helium atoms, each of which has an energy $U_{1g}^{SCF}(\infty)$,

$$\Delta U_{13g}^{SCF}(R) = U_{13g}^{SCF}(R) - 13U_{1g}^{SCF}(\infty). \tag{A1}$$

The computed $\Delta U_{13g}^{SCF}(R)$ are compared with 12 of the Hartree–Fock pair interactions in Table VI. The second nearest neighbor interactions in the 13 atom group will be negligible compared with those between nearest neighbors.

TABLE VI. Data relating energies of the 13 atom group to the pair potential.

R (a.u.)	$\Delta U_{2g}^{SCF}(R)$ (a.u.)[a]	$12\Delta U_{2g}^{SCF}(R)$ (eV)	$\Delta U_{13g}^{SCF}(R)$ (eV)[b]
5.5	0.000 037	0.0121	0.0365
6.0	0.000 011	0.0037	0.0110
6.56	0.000 004	0.0013	0.0030
7.0	0.000 001	0.0003	0.0012

[a] From Ref. 61, results labeled OSCF or AASCF.
[b] From Table B1 of Ref. 26. The data in the third column correspond to converting the literature results in the second column from atomic units to eV and multiplying by 12.

The results in Table VI confirm that our computed $\Delta U_{13g}^{SCF}(R)$ are indeed of similar magnitude to 12 times the fully optimized Hartree–Fock repulsion of just two atoms. The group energies are larger than $12\Delta U_{2g}^{SCF}(R)$ first because $\Delta U_{2g}^{SCF}(R)$ were fully optimized, thus allowing the electron densities of both atoms to be slightly displaced from their respective nuclei to minimize the Pauli type overlap repulsion. Second, the electron density of the central atom in the 13 atom group cannot relax from the spherical symmetry, except by the introduction of g orbitals, due to the very high symmetry of its environment.

For a given nuclear geometry, the total repulsion energy in the ground state of the 13 atom group, whether regarded as composed of a number of individual pair repulsions or as the prediction of the 13 atom group calculations, is very small. Any environmentally induced changes in their electron densities can be neglected. This justifies the freezing of these electron densities in the predictions of the $1s^2$ to $1s2p(^1P)$ excitation energy shifts $\Delta E(R)$ for the bulk condensed phases.

APPENDIX B: GENERATION OF CORRECT SYMMETRY EXCITED STATE GAMESS WAVEFUNCTIONS

Each molecular orbital generated by a Hartree–Fock calculation will only transform as an irreducible representation of the molecular symmetry group if the Fock Hamiltonian constructed from these orbitals transforms as the totally symmetric representation of this group. This will be the case both for a system containing shells closed only in the symmetry group but also in any symmetry group if each singly occupied orbital transforms as some one-dimensional irreducible representation. Then, the Fock Hamiltonian being constructed from quadratic products of the orbitals will be totally symmetric. However, if only one orbital from a degenerate set is occupied in a system where the symmetry group has degenerate representations, the Fock Hamiltonian will not be totally symmetric. The self-consistent field procedure will then not necessarily produce orbitals transforming as irreducible representations of the symmetry group.

The above is illustrated by the energies, $U_{13e}^{SCF}(R)$, computed using the basic model for a group of 13 helium atoms with the excited atom at the center in an environment of the approximate O_h symmetry generated by the 12 ground state atoms in the first coordinating shell. In all the calculations presented in Table VII, the eight coordinating atoms having non-zero z coordinates are located at (±6.363 961, 0, ±6.363 961 a.u.) (0, ±6.363 961, ±6.363 961 a.u.). For a structure of a full O_h symmetry, this corresponds to an R value of 9.0 a.u. Structures very similar to that of the exact O_h geometry but of a lower symmetry were generated by slight displacements of the atoms in the xy plane while retaining their zero z coordinates.

In the D_{4h} geometry generated by moving the atoms in the xy plane inward, the unpaired p electron enters the p_x orbital while moving them outward causes this electron to enter the p_z orbital. The results show that these two states are predicted to have energies differing by 0.15 eV. The computation with the electron in the non-degenerate p_z orbital of the A_{2u} symmetry is unquestionably valid because its Fock Hamiltonian is totally symmetric, thus ensuring that the entire calculation is self-consistent so far as the symmetry is concerned. This shows the calculation with the electron in the p_x orbital to be questionable. This conclusion is reinforced by the result (Table VII) that the energy predicted using the geometry of the full O_h symmetry is as much as 2.25 eV higher than that with the electron in the p_z orbital in the D_{4h} symmetry. The last three lines of Table VII present the results of three calculations performed in slightly different geometries all having the D_{2h} symmetry, this having only non-degenerate irreducible representations. Although, progressing from the fourth to the sixth line of numerical results, the electron occupies successively the p_x, p_y, and p_z orbitals, the predicted energies are not only essentially identical, but they are also the same as that predicted by the calculation of the D_{4h} symmetry with the electron in the p_z orbital. The differences in the energies predicted by these four calculations are minute as would be expected from the tiny variations between the four corresponding nuclear geometries. All the near Hartree–Fock computations in the present work were performed with small displacements of the atoms in the first coordination shell introduced to lower the symmetry to D_{2h}, thus avoiding the complications and misleading results that could arise if there were degenerate irreducible representations.

The results in Table VII show that, in the geometries of lower than the O_h symmetry, the p electron enters the orbital that is closest to a pair of atoms. This occurs because the initial estimates of the orbitals and their energies were derived by diagonalizing the one-electron Hamiltonian, the p orbital of lowest energy being that closest to the nuclei of the twelve coordinating atoms. Once this orbital is occupied with the consequent definition of the two singly occupied orbitals, the subsequent self-consistent field procedure will not change the orbital occupancies or their symmetries with the Fock matrix remaining totally symmetric. It lies beyond the scope of this paper to investigate further the difficulties arising from degenerate representations.

TABLE VII. Computed excited state energies using different symmetry groups.

Symmetry group	p electron	Coordinates of atoms in the xy plane	$U_{7e}^{SCF}(R)$
O_h	⋯	(±6.363 961, ±6.363 961, 0)	−36.373 165
D_{4h}	p_x	(±6.363 750, ±6.363 750, 0)	−36.450 600
D_{4h}	p_z	(±6.363 970, ±6.363 970, 0)	−36.455 917 24
D_{2h}	p_x	(±6.363 950, ±6.363 950 01, 0)	−36.455 917 20
D_{2h}	p_y	(±6.363 950, ±6.363 940, 0)	−36.455 917 24
D_{2h}	p_z	(±6.363 790, ±6.363 780, 0)	−36.455 917 24

APPENDIX C: THE CORRELATION ENERGIES

1. The intra-atomic correlation energies

The correlation energy of the ground state of a free helium atom is the same as its contribution to the first ionization potential as He^+ has only one electron. This energy can be derived as the difference between the experimental ionization potential[62] and the Hartree–Fock prediction[26,57] using the data assembled in Table VIII. The 1.140 eV result is very close to the value of 1.144 eV derived as the difference between the Hartree–Fock prediction for the ground state energy and the exactly computed result.[63]

Furthermore, the two electrons in the helium atom ground state are sufficiently tightly bound, in the lattice portions, that this intra-atomic correlation energy will be essentially unchanged from that in the free atom. The evidence (Appendix A) that the ground state wavefunction is essentially independent of the lattice portion density strongly indicates that the inter-atomic correlation energy will also have this property. This conclusion is supported by an analysis, to be discussed elsewhere, using a model potential for the environment of $1s^2$ electrons. It will be pointed out that although the use model potentials can often introduce significant errors, the model considered is sufficient to support the above conclusion. These observations show that the ground state correlation energy does not contribute to the excitation energy shift $\Delta E(R)$.

The difference between the Hartree–Fock energy $[U(1s2p(^1P)]$[26,65] (column 4 in Table VIII) of the $1s2p(^1P)$ state and that[26,57] (column 3) for the ground state yields the Hartree–Fock prediction of 20.115 eV for $\Delta U(\infty)$. The combination of this result with the experimental excitation value of 21.222 eV shows that the correlation contribution to this energy is 1.107 eV. The result is essentially the same as the correlation energy in the ground state. It follows that the correlation energy in this excited two-electron state is sufficiently small that it can be neglected. This conclusion is supported by the result that the exactly computed −2.123 83a.u. energy[66,67] of the free atom $1s2p(^1P)$ state is a mere 0.038 eV lower in energy than the Hartree–Fock result[26,57] of −2.122 45 a.u.

The overall conclusion is that only the ground state contributes to the non-negligible (1.11 eV Table VIII) intra-atomic correlation contribution to $\Delta U(R)$. However, the further result that this correlation energy is essentially independent of the helium atom density, as defined by R, shows that this energy does not contribute to the predictions of the energy shift $\Delta E(R)$ using (3).

2. The inter-atomic correlation energy

There is good evidence, reviewed elsewhere,[67] that as for computations of the interactions between ions in solids, the addition of the short-range correlation and dispersion energies does not introduce any significant double counting of correlation effects. This conclusion is reinforced by the later study[68] of the interactions between pairs of noble gas atoms. These systems constitute a more severe test of this conclusion because, unlike ionic crystals, these two correlation terms provide the only attractions between the atoms.

The dispersive contribution to each $\Delta E(R)$ was calculated as the difference between the values in the excited and ground states of the lattice portion. These were evaluated as the sum of all the pairwise interactions. The dipole–dipole dispersion coefficients and the parameters determining the damping at short distances are presented elsewhere.[26]

APPENDIX D: THE HELIUM DIELECTRIC CONSTANT AND WANNIER ENERGIES

The average of the experimental binding energies of the most loosely bound electron in the $1s2p(^3P)$ and $1s2p(^1P)$ states was reported in Sec. III B 1. This average was calculated from the individual binding energies (−3.623 and −3.369 eV) of these two states that in turn are derived from the 198 305 cm^{-1} ionization energy and the two excitation energies of 169 081 and 171 129 cm^{-1} from Ref. 62. As was pointed out, in Sec. III B 1, the Wannier model can only reproduce the average of the binding energies in the $1s2p(^3P)$ and $1s2p(^1P)$ states because this description does not include the exchange interaction between the two electrons. This causes the triplet and singlet levels to have electron interaction energies of J − K and J + K, respectively, in the Hartree–Fock description, where J and K are the usual direct and exchange integrals.[69] Only the J electron–electron repulsion integral enters the average of the two binding energies. For the free atom, the binding energy of the $1s2p(^1P)$ level lies at only 0.127 eV above the average energy. This difference is sufficiently small as to strongly suggest that the K integral of an atom in the condensed phase will be virtually identical to that of the free atom (the K integrals are not available individually from the computations with the GAMESS program). This conclusion taken in conjunction with the result that Hartree–Fock and Wannier predictions of the free atom average energies differ by a mere 0.095 eV allows the Wannier results $[\Delta E_W(n)]$ to be compared directly with the near Hartree–Fock values for $\Delta E(R)$. This means that $e_{2p}(0)$ in (5) should be taken to be −3.401a.u., which is the Wannier prediction for the isolated atom binding energy.

The density dependent dielectric constants presented in Table IV were derived by using the standard Clausius–Mossotti equation,

TABLE VIII. Correlation energies in the helium atom. $U[X]$ is the total electronic energy of species X.

	IP (eV)	U[$1s^2$]	U[$1s2p(^1P)$]	$\Delta U(\infty)$ (eV)
Hartree–Fock	23.447	−2.861 67 a.u.	−2.122 45 a.u.	20.115
Exact	24.587 (experiment)	−2.903 72 a.u. (calculation)	−2.123 83 a.u. (calculation)	21.22
Correlation	1.140	1.144 eV	0.038 eV	1.107

$$\frac{4\pi\alpha}{3V} = \frac{[\varepsilon(n)-1]}{[\varepsilon(n)+2]}, \tag{D1}$$

valid for high symmetry arrangements of the atoms with V being the volume occupied by one atom. The polarizability α of a single ground state helium atom in the bulk medium was taken to be the same as that (1.383a.u.[70]) of the free atom since the two 1s electrons are sufficiently tightly bound as to be essentially unaffected by their environment. An $\varepsilon(n)$ value of 1.057 has been reported[71] for the liquid at saturated vapor pressure, while the extensive compilation in Ref. 72 shows that $\varepsilon(n)$ increases with pressure with values in the range from 1.05 to 1.07 at the highest reported pressures. The comparison with these sources of experimental data validates the $\varepsilon(n)$ results presented in Table IV of the main text.

REFERENCES

[1] N. Schwentner, E.-E. Koch, and J. Jortner, *Electronic Excitations in Condensed Rare Gases* (Springer-Verlag, 1985).
[2] D. A. Arms, T. J. Graber, A. T. Macrander, R. O. Simmons, M. Schwoerer-Böhning, and Y. Zhong, Phys. Rev. B **71**, 233107 (2005).
[3] N. C. Pyper, Philos. Trans. R. Soc., A **352**, 89 (1995).
[4] G. D. Mahan, Solid State Ionics **1**, 29 (1980).
[5] Z. K. Tang, Y. Nozue, and T. Goto, J. Phys. Soc. Jpn. **61**, 2943 (1962).
[6] B. D. Perlson and J. A. Weil, J. Magn. Reson. **15**, 594 (1974).
[7] S. N. Foner, E. L. Cochran, V. A. Bowers, and C. K. Jen, J. Chem. Phys. **32**, 963 (1960).
[8] J.-P. Connerade, V. K. Dolmatov, and S. T. Manson, J. Phys. B: At., Mol. Opt. Phys. **32**, L395 (1999).
[9] N. Aquino, Adv. Quantum Chem. **57**, 123 (2009), and references cited therein.
[10] B. M. Gimarc, J. Chem. Phys. **47**, 5110 (1967).
[11] E. V. Ludeña, J. Chem. Phys. **69**, 1770 (1978).
[12] A. D. Sañu-Ginarte, L. Ferrer-Galindo, R. A. Rosas, A. Corella-Madueno, R. Betancourt-Riera, L. A. Ferrer-Moreno, and R. Riera, J. Phys. Commun. **2**, 015001 (2008).
[13] V. K. Dolmatov, Adv. Quantum Chem. **58**, 13 (2009).
[14] J. C. A. Boeyens, J. Chem. Soc., Faraday Trans. **90**, 3377 (1994).
[15] M. Rahm, R. Cammi, N. W. Ashcroft, and R. Hoffmann, J. Am. Chem. Soc. **141**, 10253 (2019).
[16] L. F. Pašteka, T. Helgaker, T. Saue, D. Sundholm, H.-J. Werner, M. Hasanbulli, J. Major, and P. Schwerdtfeger, Mol. Phys. **118**, e1730989 (2020).
[17] E. Ley-Koo and S. Rubinstein, J. Chem. Phys. **71**, 351 (1979).
[18] J. Gorecki and W. B. Brown, J. Phys. B: At., Mol. Opt. Phys. **21**, 403 (1988).
[19] P. W. Fowler and P. A. Madden, Mol. Phys. **49**, 913 (1983).
[20] P. W. Fowler and P. A. Madden, Phys. Rev. B **29**, 1035 (1984).
[21] P. W. Fowler and P. A. Madden, J. Phys. Chem. **89**, 2581 (1985).
[22] E. Bichoutskaia and N. C. Pyper, J. Phys. Chem. C **111**, 9548 (2007), also references cited therein.
[23] P. W. Fowler, P. J. Knowles, and N. C. Pyper, Mol. Phys. **56**, 83 (1985).
[24] N. C. Pyper, A. I. Kirkland, and J. H. Harding, J. Phys.: Condens. Matter **18**, 683 (2006), also references cited therein.
[25] A. A. Lucas, J. P. Vigneron, S. E. Donnelly, and J. C. Rife, Phys. Rev. B **28**, 2485 (1983).
[26] N. C. Pyper, D. W. Essex, and C. T. Whelan, Philos. Mag. B **81**, 91 (2001).
[27] N. C. Pyper, T. C. Naginey, P. D. Nellist, and C. T. Whelan, Philos. Mag. Lett. **97**, 295 (2017).
[28] C. M. Surko, G. J. Dick, F. Reif, and W. C. Walker, Phys. Rev. Lett. **23**, 842 (1969).
[29] N. Schell, R. O. Simmons, A. Kaprolat, W. Schülke, and E. Burkel, Phys. Rev. Lett. **74**, 2535 (1995).
[30] D. A. Arms, Ph.D. thesis, University of Illinois at Urbanna Champaign, 1999.
[31] D. A. Arms, R. O. Simmons, M. Schwoerer-Böhning, A. T. Macrander, and T. J. Graber, Phys. Rev. Lett. **87**, 156402 (2001).
[32] J. D. Sugar, R. D. Twesten, N. C. Bartelt, C. A. Taylor, N. R. Catarineu, and D. B. Robinson, Microsc. Microanal. **24**(S1), 438 (2018).
[33] M.-L. David, F. Pailloux, V. Mauchamp, and L. Pizzagalli, Appl. Phys. Lett. **98**, 171903 (2011).
[34] K. Alix, M.-L. David, G. Lucas, D. T. L. Alexander, F. Pailloux, C. Hébert, and L. Pizzagalli, Micron **77**, 57 (2015).
[35] D. Taverna, M. Kociak, O. Stephan, A. Fabre, E. Finot, B. Déscamps, and C. Colliex, Phys. Rev. Lett. **100**, 035301 (2008).
[36] C. A. Walsh, J. Yuan, and L. M. Brown, Philos. Mag. A **80**, 1507 (2000).
[37] S. Fréchard, M. Walls, M. Kociak, J. P. Chevalier, J. Henry, and D. Gorse, J. Nucl. Mater. **393**, 102 (2009).
[38] N. C. Pyper, C. G. Pike, P. Popelier, and P. P. Edwards, Mol. Phys. **86**, 995 (1995).
[39] M.-S. Miao and R. Hoffmann, Acc. Chem. Res. **47**, 1311 (2014).
[40] R. Schierholz, B. Lacroix, V. Godinho, J. Caballero-Hernández, M. Duchamp, and A. Fernández, Nanotechnology **26**, 075703 (2015).
[41] A.-M. Seydoux-Guillaume, M.-L. David, K. Alix, L. Datas, and B. Bingen, Earth Planet. Sci. Lett. **448**, 133 (2016).
[42] M. Klimenkov, A. Möslang, and E. Materna-Morris, Micron **46**, 51 (2013).
[43] A. Boatwright, C. Feng, D. Spence, E. Latimer, C. Binns, A. M. Ellis, and S. Yang, Faraday Discuss. **162**, 113 (2013).
[44] See the discussion in Ref. 45 of Fig. 6 in Ref. 25.
[45] J. S. Dugdale and F. E. Simon, Proc. R. Soc. London **218**, 291 (1953).
[46] R. L. Mills and A. F. Schuch, Phys. Rev. Lett. **6**, 263 (1961).
[47] R. Boehm and R. Yaris, J. Chem. Phys. **55**, 2620 (1971).
[48] R. G. Gordon and Y. S. Kim, J. Chem. Phys. **56**, 3122 (1972).
[49] N. Jacobi and G. Csanak, Chem. Phys. Lett. **30**, 367 (1975).
[50] E. C. Svensson, V. F. Sears, A. D. B. Woods, and P. Martel, Phys. Rev. B **21**, 3638 (1980).
[51] H. N. Robkoff and R. B. Hallock, Phys. Rev. B **25**, 1572 (1982).
[52] C. T. Venkataraman and R. O. Simmons, Rev. Sci. Instrum. **67**, 3365 (1996).
[53] A. P. M. Glassford and J. L. Smith, Cryogenics **6**, 193 (1966).
[54] H. K. Mao, E. L. Shirley, Y. Ding, P. Eng, Y. Q. Cai, P. Chow, Y. Xiao, J. Shu, R. J. Hemley, C. Kao, and W. L. Mao, Phys. Rev. Lett. **105**, 186404 (2010).
[55] H. A. Bethe and E. E. Salpeter, *Quantum Mechanics of One- and Two-Electron Atoms* (Plenum/Roseta, 1977), p. 17, Eq. (3.21) with $Z = e = 1$.
[56] C. Froese-Fischer, *The Hartree-Fock Method for Atoms: A Numerical Approach* (Wiley, 1977), Table 4.10, p. 175.
[57] H. A. Bethe and E. E. Salpeter, *Quantum Mechanics of One- and Two-Electron Atoms* (Plenum/Roseta, 1977), p. 17, Eq. (3.20).
[58] M. Inokuti, Rev. Mod. Phys. **43**, 297 (1971).
[59] B. H. Bransden and C. J. Joachain, *Physics of Atoms and Molecules* (Prentice-Hall, Harlow, 2003).
[60] M. F. Guest, I. J. Bush, H. J. J. van Dam, P. Sherwood, J. M. H. Thomas, J. H. van Lenthe, R. W. A. Havenith, and J. Kendrick, Mol. Phys. **103**, 719 (2005), GAMESS-UK is a package of *ab initio* programs. See http://www.cfs.dl.ac.uk/gamess-uk/index.shtml.
[61] T. L. Gilbert and A. C. Wahl, J. Chem. Phys. **47**, 3425 (1967).
[62] C. E. Moore, *Atomic Energy Levels* (National Bureau of Standards, Washington, DC, 1949), Vol. 1.
[63] C. L. Pekeris, Phys. Rev. **115**, 1216 (1959).
[64] C. Froese-Fischer, *The Hartree-Fock Method for Atoms: A Numerical Approach* (Wiley, 1977), Table 2.3, p. 28.
[65] Y. Accad, C. L. Pekeris, and B. Schiff, Phys. Rev. A **4**, 516 (1971).
[66] C. F. Fischer and K.-t. Cheng, J. Phys. B: At. Mol. Phys. **15**, 337 (1982).

[67]N. C. Pyper, Adv. Solid State Chem. **2**, 223 (1991), also references cited therein.
[68]M. P. Housden and N. C. Pyper, Mol. Phys. **105**, 2353 (2007).
[69]C. T. Whelan, *Atomic Structure* (IOP/Morgan and Claypool, 2018).
[70]T. M. Miller and B. Bederson, Adv. At. Mol. Phys. **13**, 1 (1977), Table 1.
[71]R. J. Donnelly and C. F. Barenghi, J. Phys. Chem. Ref. Data **27**(6), 1217 (1998).
[72]*CRC Handbook of Physics and Chemistry*, 97th ed., edited by W. M. Haynes (CRC Press, Boca Raton, 2016), 6-28 and 6-29.